Article:
Shashkova, Sviatlana, Nyström, Thomas, Leake, Mark Christian et al. (2020) Correlative single-molecule fluorescence barcoding of gene regulation in Saccharomyces cerevisiae. Methods. ISSN: 1046-2023

https://doi.org/10.1016/j.ymeth.2020.10.009

Methods 193 (2021) 46–53

Contents lists available at ScienceDirect

Methods

journal homepage: www.elsevier.com/locate/ymeth

Correlating single-molecule characteristics of the yeast aquaglyceroporin Fps1 with environmental perturbations directly in living cells

Sviatlana Shashkova [a,*,1,2], Mikael Andersson [b,1], Stefan Hohmann [c], Mark C. Leake [a,2]

[a] Department of Physics, University of York, YO10 5DD York, UK
[b] Department of Chemistry and Molecular Biology, University of Gothenburg, 405 30 Gothenburg, Sweden
[c] Department of Biology and Biological Engineering, Chalmers University of Technology, 412 96 Gothenburg, Sweden

ARTICLE INFO

Keywords:
Plasma membrane channels
Single-molecule
Super-resolution
Living cell
Osmotic condition
Cell stress

ABSTRACT

Membrane proteins play key roles at the interface between the cell and its environment by mediating selective import and export of molecules via plasma membrane channels. Despite a multitude of studies on transmembrane channels, understanding of their dynamics directly within living systems is limited. To address this, we correlated molecular scale information from living cells with real time changes to their microenvironment. We employed super-resolved millisecond fluorescence microscopy with a single-molecule sensitivity, to track labelled molecules of interest in real time. We use as example the aquaglyceroporin Fps1 in the yeast *Saccharomyces cerevisiae* to dissect and correlate its stoichiometry and molecular turnover kinetics with various extracellular conditions. We show that Fps1 resides in multi tetrameric clusters while hyperosmotic and oxidative stress conditions cause Fps1 reorganization. Moreover, we demonstrate that rapid exposure to hydrogen peroxide causes Fps1 degradation. In this way we shed new light on aspects of architecture and dynamics of glycerol-permeable plasma membrane channels.

1. Introduction

Traditional techniques in biochemistry and molecular biology are usually performed on a population ensemble average level. Such approaches "smooth" the noise by averaging the observations from anomalous outlying units. Every population under investigation, whether it is a cell culture or a protein bulk within a unicellular organism, is a heterogeneous system. Therefore, ensemble averaging masks important effects of subpopulations [1–3], such as drug resistant bacteria or cancer cells [4–6]. Single-molecule optical biophysics methods permit real-time visualization of key cellular processes [7], the action of so-called biological 'nanomachines' [8], such as signal transduction, gene expression, immune response, mapping cellular genome, etc., providing direct insights into molecular mobility, stoichiometry, copy numbers [9,10]. Novel localization-based super-resolved microscopy techniques allow tracking individual molecules of the same type (e.g. FliM protein of *Escherichia coli* [8]) or different types (e.g. correlating separate motions of proteins and lipids in the same bacteria cell [11]) to uncover "hidden" subpopulations, thus, determining precise biological functions [9].

An important part in understanding the regulation of a membrane protein is revealing its dynamics of within the membrane, interaction with other proteins, re-localization and turnover [9]. One of the most frequently used super-resolution methods for plasma membrane protein studies is total internal reflection fluorescence (TIRF) due to its relative simplicity to setup to enable selective illumination and excitation of fluorophores positioned close to the cover slip. Photoactivated localization microscopy (PALM) and stochastic optical reconstruction

Abbreviations: dNTP, deoxyribonucleotide triphosphate; DTT, dithiothreitol; EDTA, ethylenediaminetetraacetic acid; EGTA, egtazic acid; EMCCD, electron multiplying charge-coupled device; GFP, green fluorescent protein; MIP, major intrinsic protein; PBS, phosphate-buffered saline; PCR, polymerase chain reaction; SDS, sodium dodecyl sulfate; TIRF, total internal reflection fluorescence; YNB, yeast nitrogen base; YPD, yeast extract peptone dextrose.

* Corresponding author at: Department of Microbiology and Immunology, Institute for Biomedicine, Sahlgrenska Academy, University of Gothenburg, 405 30 Gothenburg, Sweden.

E-mail addresses: sviatlana.shashkova@york.ac.uk (S. Shashkova), mikael.andersson.2@gu.se (M. Andersson), stefan.hohmann@chalmers.se (S. Hohmann), mark.leake@york.ac.uk (M.C. Leake).

[1] These authors contributed equally.
[2] Department of Biology, University of York, YO10 5DD York, UK.

https://doi.org/10.1016/j.ymeth.2020.05.003
Received 28 February 2020; Received in revised form 4 May 2020; Accepted 4 May 2020
Available online 6 May 2020

microscopy (STORM) have a wide range of applications including membrane protein investigations too [4]. Conventional PALM and STORM utilize a photoconversion process of the fluorophore and involve reconstruction over normally thousands of consecutive image frames. These techniques have a typical effective temporal resolution of 0.5–1 s which provides limitations in studying fast dynamic processes in living cells [12,13]. However, more rapid sptPALM approaches have recently been employed to monitor dynamics with a time resolution of a few tens of ms per frame [14].

The plasma membrane is a selectively-permeable natural barrier that ensures cell homeostasis via controlling among others nutrient sensing and uptake as well as flux of metabolites [15–17]. The Fps1 protein of the budding yeast *Saccharomyces cerevisiae* is a gated aquaglyceroporin, a member of the major intrinsic protein (MIP) family of plasma membrane channel proteins. The primary purpose of Fps1 is to mediate the efflux of glycerol to regulate cellular turgor pressure [18]. Fps1 is actively regulated in response to hyper and hypo-osmotic stress, or presence of compounds in the environment to which Fps1 is permeable [18–21].

Studies on Fps1 channel stoichiometry via co-immunoprecipitation followed by SDS-PAGE separation and immunoblot analysis suggest that Fps1 exists as a monomer but may also self-associate into multimeric complexes with up to four Fps1 molecules [22]. Structural analyses on other MIP members, canonically water permeable aquaporins [23], indicate a tetrameric organization where each monomer defines a pore with a possible fifth pore formed in the center of the tetramer [24]. However, the aspects of MIP channels assembly, architecture and dependencies of their regulation in living cells on the microenvironment, remain to be elucidated.

Here, we employ single-molecule Slimfield super-resolved fluorescence microscopy on GFP-tagged yeast Fps1 to reveal new aspects of the MIP proteins organization and regulation which links directly to their function and, importantly, correlate our observations to changes in the extracellular microenvironment. Slimfield is a powerful optical microscopy tool that uses spatially delimited illumination confined to vicinity of approximately a single cell and enables millisecond imaging of fluorescent protein fusions directly in living cells [25–27]. We have also combined this technique with deconvolution analysis to calculate Fps1 copy numbers. Our study provides novel insights into understanding of cellular adaptation to the microenvironment through characterization of the plasma membrane channels.

2. Materials and methods

2.1. Growth conditions and media

Cells from frozen stocks were pre-grown on standard YPD medium (20 g/L Bacto Peptone, 10 g/L Yeast Extract) supplemented with 2% glucose (w/v) at 30 °C overnight. For liquid cultures, cells were grown in Yeast Nitrogen Base (YNB) medium (1× Difco™ YNB base, 1× Formedium™ complete amino acid Supplement Mixture, 5.0 g/L ammonium sulfate, pH 5.8–6.0) supplemented with 2% glucose (w/v) and 1 M sorbitol if required, at 30 °C, 180 rpm.

For microscopy experiments, cells were pre-grown overnight in YNB media with 20 g/L glucose and grown until mid-logarithmic phase, OD_{600} 0.4–0.7. For sorbitol experiments, all media were supplemented with 1 M sorbitol throughout the whole process to reach full osmoadaptation to the high osmolarity. For oxidative stress experiments, cultures were treated with 0.4 mM H_2O_2 immediately prior to imaging. Cells were then immobilized by placing 5 μL of the cell culture onto a 1% agarose pad perfused with YNB supplemented with 2% glucose (w/v) and 1 M sorbitol or 0.4 mM H_2O_2. The pad with cells was sealed with a plasma-cleaned BK7 glass microscope coverslip (22 × 50 mm).

2.2. Strain construction

To prevent artificial aggregation of GFP, we used a variant (further denoted as mGFP) containing a A206K mutation to discourage self-oligomerization, as well as S65T and S72A mutations to improve protein photostability and fluorescence output [4,28,29]. Although within protein fusions, large fluorescent proteins may disturb physiological behavior of a protein under investigation, functionality of fluorescently labelled Fps1 has been previously confirmed [19,30–32].

mGFP-HIS3 fragment from pmGFP-S plasmid [33], flanked with 50 bp up- and downstream the STOP codon of the *FPS1* gene on 5′ and 3′ ends, respectively, was amplified by PCR using 200 μM of each dNTP, forward and reverse primers 0.5 μM each, 1x Phusion HF buffer (Thermo Scientific), 0.02 U/μL Phusion™ High-Fidelity DNA Polymerase (Thermo Scientific) reaction mix (for PCR program details see Supplementary Table 1) and purified with QIAquick PCR Purification Kit (QIAGEN). The Fps1-mGFP strain was created by transforming the BY4741 background strain with 100 μL of the purified *mGFP-HIS3* fragment with standard LiAc protocol to allow for homologous recombination [34]. Successful clones were verified by the confirmation PCR and standard epifluorescence microscopy. PCR primers used in this study are listed in Supplementary Table 2.

2.3. 4 Single-molecule Slimfield microscopy

Slimfield excitation was implemented via 50mW 473 nm wavelength laser (Vortran Laser Technology, Inc.) de-expanded to direct a beam onto the sample at 15mW excitation intensity to observe single GFP in living yeast cells [33]. Fluorescence emission was captured by a 1.49 NA oil immersion objective lens (Nikon) followed by 300 mm focal length tube lens (Thorlabs) [10]. Images were collected at 5 ms exposure time every 10 ms by Photometrics Evolve 512 Delta EMCCD camera using 93 nm/pixel magnification.

The focal plane was set to mid-cell height using the brightfield appearance of cells. As photobleaching of mGFP proceeded during Slimfield excitation distinct fluorescent foci could be observed of half width at half maximum 250–300 nm, consistent with the diffraction-limited point spread function of our microscope system, which were tracked and characterized in terms of their stoichiometry and apparent microscopic diffusion coefficient. Distinct fluorescent foci that were detected within the microscope's depth of field could be tracked for up to several hundred ms, to a super-resolved lateral precision ~40 nm [35] using a bespoke single particle tracking software written in MATLAB (MATHWORKS) and adapted from similar live cell single-molecule studies [10,35–37].

The molecular stoichiometry for each track was determined by dividing the summed pixel intensity values associated with the initial unbleached brightness of each foci by the brightness corresponding to that calculated for a single fluorescent protein molecule (mGFP for 473 nm wavelength excitation) measured using a step-wise photobleaching technique described elsewhere [33,38]. The apparent microscopic diffusion coefficient D was determined for each track by calculating the initial gradient of the relation between the mean square displacement with respect to tracking time interval using the first 10 time intervals values while constraining the linear fit to pass through $4\sigma^2$ on the vertical axis corresponding to a time interval value of zero. Maturation effects of fluorescent protein fusions withing living cells were characterized on similar yeast cell lines previously, indicating typically 10–15% immature 'dark' fluorescent protein [39].

Similar to molecular stoichiometry calculations, total numbers of Fps1-mGFP were estimated based on the background- and autofluorescence corrected integrated density values of each cell as well as fluorescence intensity of a single fluorophore obtained through ImageJ Fiji Software.

3. Protein extracts preparation and immunoblotting

Cells were grown in 100 mL of YNB medium supplemented with 4% glucose at 30 °C, 180 rpm. When OD_{600} reached 0.8, 50 mL was transferred to a new flask and subjected to 0.4 mM H_2O_2 for 1 h while the remaining 50 mL were kept untreated as a control. Cells were harvested by centrifugation (2000g, 10 min) and washed in 10 mL of a wash buffer (10 mM TrisHCl pH 7.5, 0.5 M sucrose, 2.5 mM EDTA), and in 20 mL of ice cold homogenization buffer (50 mM TrisHCl pH 7.5, 0.3 M sucrose, 5 mM EDTA, 1 mM EGTA, 2 mM DTT, 1× protease inhibitor (cOmplete EDTA free, Roche)). To obtain lysates, cells were resuspended in 0.5 mL of ice cold homogenization buffer with an addition of 0.5 mL of acid washed glass beads, and disrupted at 4 °C with a FastPrep-24™ instrument (MP-Biomedicals) in 3 × 20 s cycles (speed 6.0 m/s, 5 min rest on ice between each cycle). Lysates were cleared via centrifugation (10 000g, 10 min, 4 °C), and the supernatant was centrifuged again (100 000g, 1 h, 4 °C). Pellets were washed with a membrane wash buffer (10 mM TrisHCl pH 7.0, 1 mM EGTA, 1 mM DTT, 1x protease inhibitor), repelleted via centrifugation (40 000g, 1 h, 4 °C) and dissolved in 100 μL of ice-cold membrane wash buffer. The total protein concentration was determined via UV–Vis (Nanodrop 1000, Thermo Fisher Scientific). Prior to SDS-page, protein extracts were mixed with Laemmli buffer [40] and heated at 95 °C for 5 min. Separation was done via SDS-page (4–15% Criterion™ TGX™ Precast Midi Protein Gel, Bio-Rad Laboratories) with equal amounts of total protein per well for all sample pairs. Resolved proteins were transferred onto a nitrocellulose membrane (0.2 μm NC, Bio-Rad Laboratories) using a Trans-Blot Turbo (Bio-Rad Laboratories). The membrane was blocked for 1 h with an Intercept PBS blocking buffer (LI-COR biosciences) and incubated with a primary antibody (mouse anti-GFP (Roche), 1:10 000 dilution in the Intercept PBS blocking buffer) for 15 h at 4 °C. The membrane was then washed 5 × 5 min with PBSt (PBS buffer with 0.1% Tween-20) and incubated with the secondary antibody (IRDye 800CW goat anti-mouse, 1:20 000 dilution in Intercept PBS blocking buffer) at the room temperature for 1 h followed by washing with PBSt as indicated above. Prior to imaging, the membrane was washed 2 × 5 min with PBS. Signals were visualized using an Odyssey IR scanner (LI-COR Biosciences). Band intensity was quantified with Image-Studio Lite (LI-COR Biosciences) using local background normalization.

4. Results and discussion

4.1. Fps1 resides in multi tetrameric assemblies

In both eukaryotes and prokaryotes, aquaglyceroporins have been reported to act as tetramers [41–44]. To visualize and further investigate previous reports on Fps1 tetramerization [22], we employed single-colored single-molecule fluorescence Slimfield super-resolution microscopy (Fig. 1A) to determine the stoichiometry of the GFP-tagged yeast Fps1 under non-stressed conditions (Fig. 1B, top panel, Supplementary Video 1). We acquired about 500 frames per field of view at the rate of 200 frames per second, and applied a bespoke MATLAB code [33,35] to identify all bright spots in each frame and link them to spots in neighboring frames in order to build trajectories. The stoichiometry of each fluorescent spot was identified by comparing its fluorescent intensity with that corresponding to a single GFP molecule. Consistent with previously published data and observations of aquaporins in other eukaryotes, Fps1 seems to be present as tetramers, which are also organized in higher stoichiometry spots (Fig. 1C). Based on the previous estimation of the *S. cerevisiae* plasma membrane width [45], we accepted any GFP tracks found between the cell boundaries identified from the brightfield image and *ca.* 7 nm into the cell as the plasma membrane foci, henceforth referred to as membrane, while the spots found in the rest of the cell as “intracellular”. The mean apparent

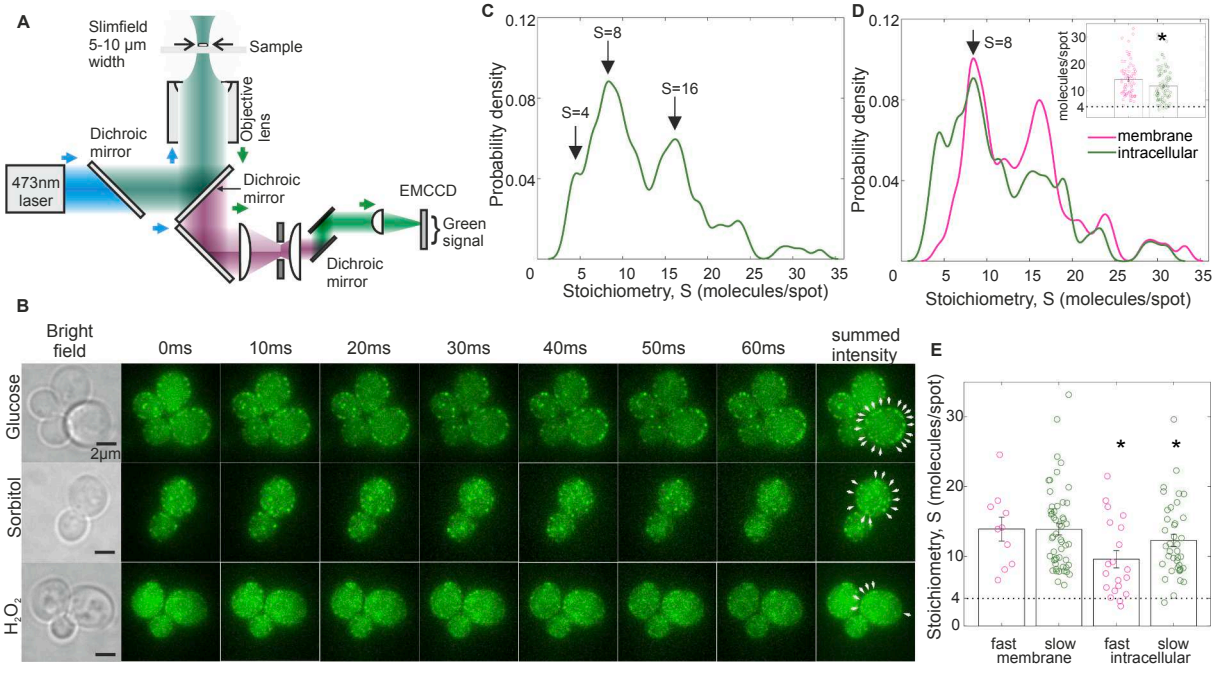

Fig. 1. A. Single-colored Slimfield super-resolved microscopy setup. B. Examples of Slimfield images of *S. cerevisiae* cells expressing genomically integrated Fps1-mGFP fusion under non-stressed conditions (top panel, glucose), hyper-osmotic conditions (middle panel, sorbitol) and 30 min oxidative stress (bottom panel, H_2O_2): brightfield and green channel (right) are shown. White arrows point at the fluorescent foci located in the cell membrane. Scale bar 2 μm. C. Kernel Density Estimation plot (kernel width = 0.7) of the Fps1-mGFP stoichiometry distribution under non-stressed conditions (n = 40 cells). D. Kernel Density Estimation plots of the Fps1-mGFP stoichiometry distributions on the cellular membrane (magenta) and intracellular (green) spots. Inset: Jitter plots of membrane (magenta) and intracellular (green) Fps1-mGFP foci stoichiometry. Error bars represent standard error of mean. Student *t*-test, *p < 0.05. E. Jitter plots of apparent stoichiometries of fast moving (fast), diffusion coefficient, $D > 0.8$ μm^2/s, and immobile, $D < 0.3$ μm^2/s, (slow) membrane and intracellular Fps1-mGFP foci. Standard error bars are indicated. Student *t*-test, *p < 0.05.

stoichiometry of the membrane foci is higher compared to those found in the rest of the cell (14 ± 6.2 and 12 ± 6.3, respectively. Student *t*-test. Fig. 1D). Unlike membrane Fps1, intracellular spots seem to be also present as lower stoichiometry oligomers (Fig. 1D, inset, and 1E). Foci of the same stoichiometry can be both immobile (diffusion coefficient, $D < 0.3\ \mu m^2/s$) and fast moving ($D > 0.8\ \mu m^2/s$) (Fig. 1E). Other aquaporins are known to reside in intracellular storage vesicles or lipid rafts until they are required at the plasma membrane [46–48]. The abundance of intracellular Fps1 suggests that it could also reside in such vesicles. Key glycerol metabolizing enzymes are located in subcellular compartments, such as mitochondria, peroxisomes and lipid droplets [49–51]. Thus, intracellular Fps1 might be sitting on their membranes where it mediates the flux for a substrate. Some aquaporins have been shown to be present in the secretory vesicles membranes [52]. Although Fps1 also seems to be present in these organelles, the amounts have been suggested to be low and most likely not functional [53].

Interestingly, the mean apparent stoichiometry of the fast moving and immobile membrane foci is also similar (Fig. 1E). The limitation of our segmentation method is that budding cells are accepted as two separate cells with the "whole-cell" plasma membrane without accounting for the mother-daughter cell connection through the bud neck. Therefore, the mobile pool might represent Fps1 located closer to the bud, where proteins can move between the mother and the daughter cells, which would be consistent with previous reports on multiple plasma membrane proteins are asymmetrically segregated [54]. However, further studies with bud neck labelling should be performed to verify that.

4.2. Sorbitol causes a change in Fps1 organization

Biochemical studies suggest that increased external osmolarity causes rapid Fps1 closure, whereas decreased osmolarity results in the channel opening [30,55,56]. To determine how hyper-osmotic conditions affect Fps1 architecture, we grew the cells in 1 M sorbitol to reach complete osmoadaptation (Fig. 2A and Fig. 1B, middle panel, Supplementary Video 2). Sorbitol growth causes the apparent stoichiometry shift towards higher oligomeric clusters (Fig. 2B) with the highest probability peak of 8 molecules/spot in the absence of sorbitol (Fig. 1B) and 11 molecules/cell in sorbitol (Fig. 2C). Sorbitol had been shown to increase molecular crowding in cells [57,58]. The Fps1 protein contains 11 regions with intrinsic disorder making an overall proportion of disordered content >44%, >71% of which is within the large N- and C-terminal cytoplasmic domains (as predicted by PONDR software). Disordered motifs may undergo phase transition resulting in formation of higher oligomers, in this case, facilitated by increased intracellular crowding [33]. These cytoplasmic domains are however also shown to be the main facilitators of protein interaction with Fps1 [19,31,59–61]. Computer simulations indicate that specific protein interactions can also be stabilized upon an increase in molecular crowding [62]. This together with known interactions with of Fps1 in membrane bound signal scaffolding is also likely to affect Fps1 stoichiometry [59]. No clear periodicity of four Fps1 molecules/spot was found in sorbitol-grown cells. The overall stoichiometry spread is much broader compared to that found in glucose (Fig. 2B, inset) regardless of the foci localization, indicating a range from Fps1 dimers up to 50 molecules/spot (Fig. 2C, inset).

Increased crowding also results in lower mean diffusion coefficient, *D*: 0.43 ± 0.61 $\mu m^2/s$ in non-stress conditions as opposed to 0.36 ± 0.51 $\mu m^2/s$ upon hyper-osmotic environment (Fig. 2D). However, no obvious linear correlation between the diffusion coefficient and foci stoichiometry was observed in normal and stress conditions (Fig. 3). According with our expectation that molecular movement is more restricted in the membrane, only few of the "fast" spots ($D > 0.8\ \mu m^2/s$) are found on the membrane under both non-stress (glucose) and sorbitol conditions (Fig. 3 top left and bottom left). "Immobile" foci ($D < 0.3\ \mu m^2/s$) are equally present on the membrane and in the rest of the cell (Fig. 3 top right and bottom right). Interestingly, spots with the lowest *D* are not actually the ones of the highest stoichiometry. This suggests that Fps1 is trafficked, and thereby also likely regulated, as a multimer. Alternatively, Fps1 trafficking and regulation might also occur as part of a complex with other proteins or as part of a mobile membrane compartment.

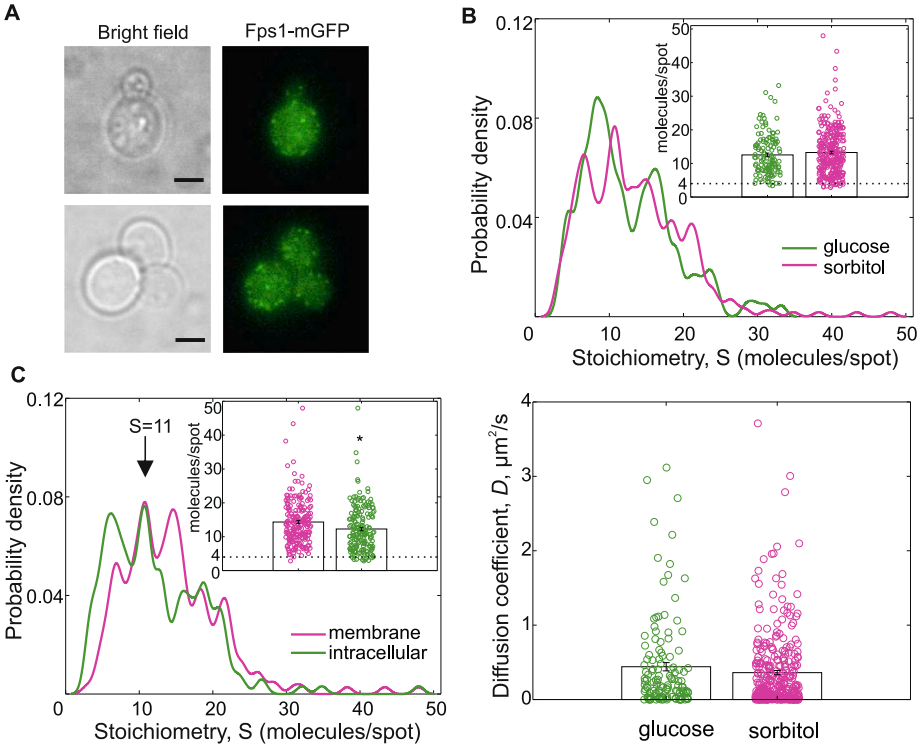

Fig. 2. A. Examples of Slimfield images of *S. cerevisiae* cells expressing genomically integrated Fps1-mGFP fusion under hyper-osmotic stress (media supplemented with 1 M Sorbitol): brightfield (left) and green channel (right) are shown. Scale bar 2 μm. B. Kernel Density Estimation plot (kernel width = 0.7) of the Fps1-mGFP stoichiometry distributions upon normal (green, n = 40 cells) and hyper-osmotic stress (magenta, n = 89 cells) conditions. Inset: Jitter bar chart of mean apparent stoichiometry, standard error of mean error bars are shown. C. Kernel Density Estimation plots of the Fps1-mGFP stoichiometry distributions on the cellular membrane (magenta) and intracellular (green) spots. Inset: Jitter plot of membrane (magenta) and intracellular (green) Fps1-mGFP foci stoichiometry. Error bars represent standard error of mean. Student *t*-test, *p < 0.05. D. Jitter plot of the mean diffusion coefficients of Fps1-mGFP foci under normal (glucose, green) and hyper-osmotic (sorbitol, magenta) conditions. Error bars represent standard error of mean.

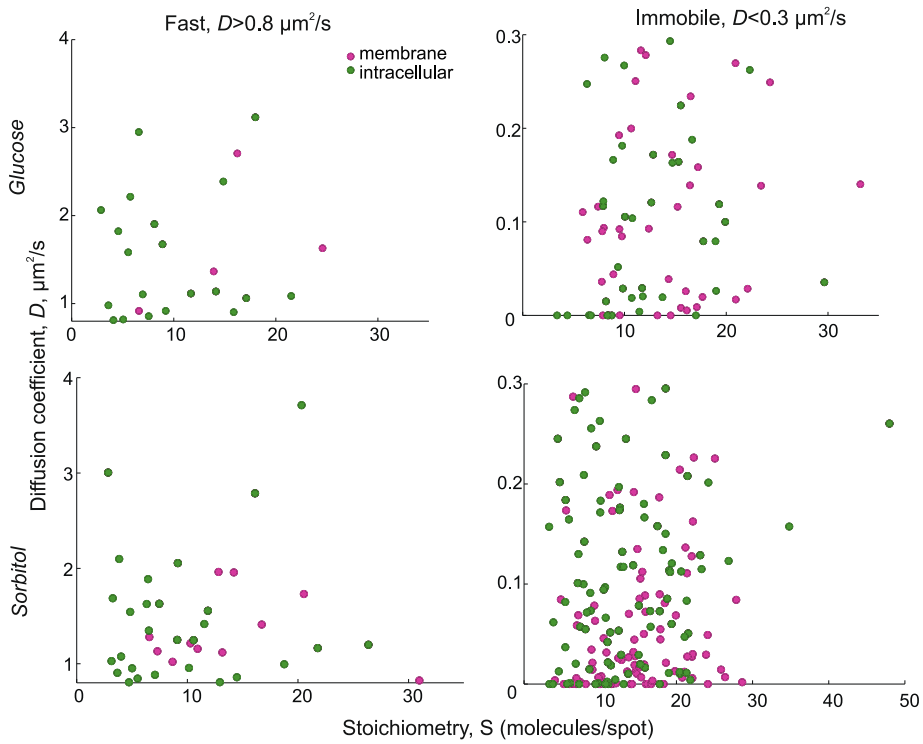

Fig. 3. Scatter plots of stoichiometry and diffusion of fast, $D > 0.8$ μm^2/s (left), and immobile, $D < 0.3$ μm^2/s (right), Fps1-mGFP spots found on the membrane (magenta) and the rest of the cell (green) upon non-stress (top) and hyper-osmotic (bottom) conditions.

4.3. Oxidative stress rapidly facilitates Fps1 degradation

MIPs have been shown to facilitate hydrogen peroxide diffusion through cell membranes [63–65]. To study the effect of the rapid exposure to the oxidative stress on Fps1 composition, we treated cells with 0.4 mM H_2O_2 for 20–40 min prior to imaging (Fig. 1B, bottom panel, Fig. 4A, Supplementary Video 3). No significant differences could be found in mean apparent stoichiometry and diffusion coefficients between all three conditions (Fig. 4B). Similar to that, upon sorbitol treatment, regardless of the cellular compartment, Fps1 exists as a dimer (Fig. 4C).

We identified three times less Fps1 molecules in cells exposed to H_2O_2 compared to those incubated in non-stress conditions (Fig. 4D). Hydrogen peroxide can induce protein internalization or degradation in various organisms – in plants, aquaporins have been shown to internalize upon H_2O_2 and salt treatment [47,65], degradation has been demonstrated for hemoglobin and membrane proteins in mammals [66] and intracellular proteins in *E. coli* [67]. Fps1 has been suggested to undergo endocytosis in response to acetate-induced oxidative stress [19,68]. To investigate the effect of hydrogen peroxide-induced oxidative stress on Fps1, we performed western blotting on protein extracts from cells exposed to H_2O_2 (Fig. 4E). Quantification of the signal indicated that the protein band intensity from cells after the stress is only 65% of that from untreated cells suggesting the role of hydrogen peroxide in Fps1 degradation.

The presence of dimers during both sorbitol growth and H_2O_2 stress, together with lower copy numbers of Fps1 molecules (Fig. 4D), point towards differences in protein turnover during these conditions compared to the standard environment. Dimerization as an intermediate state has already been reported for MIPs in other organisms. For example, the tetramer of the *E. coli* aquaglyceroporin GlpF unfolds via a dimeric intermediate state [69]. In plants, there is also evidence of constitutive aquaporin cycling which has been theorized to favor the plasticity of the channel activity and its response to sudden environmental changes [47]. The dimerization of plant aquaporins is thought to stabilize the channel in the membrane [70–73]. Thus, the different range of Fps1 stoichiometries under stress conditions indicates changes in protein turnover leading in the case of H_2O_2 to degradation.

To determine if the Fps1 spots' behavior changes over time, we split the acquired dataset into three groups representing cells being exposed to the oxidative stress for 20, 30 or 40 min. Consistently with our expectations, the mean apparent stoichiometry of Fps1-mGFP seems to decrease over time (Fig. 4F top). Interestingly, the smallest stoichiometry number increases across all three groups, from two molecules/spot in group 1 (20 min of H_2O_2 treatment) to four in group 3 (40 min). While no difference in the mean diffusion coefficient was identified between three groups (Fig. 4F bottom), the number of fast moving ($D > 0.8$ μm^2/s) Fps1 foci identified in group 3 cells (40 min of hydrogen peroxide treatment) is significantly smaller (Fig. 4G). Together, these findings point towards the initial assembly of smaller foci into larger stoichiometry spots which are further subjected to hydrogen peroxide-induced degradation.

5. Conclusions

In 1972 the idea that the cell membrane was a fluid two dimensional lipid bilayer was introduced [74]. Since then our knowledge of the plasma membrane and its components has increased exponentially and we know that it is a complex and dynamic network of lipids and proteins that can cluster and confer general and localized properties in both two and three dimensions [75,76]. These protein clusters can either be stable or exist more transiently [77,78] and facilitate various cellular processes, such as signal transduction and gene regulation via recruitment of protein complex components to target DNA and channel activators to the plasma membrane [31,33].

Here we show that the yeast aquaglyceroporin Fps1 on the membrane is organized into multimeric clusters of varying sizes. Our data show that the oligomerization state of Fps1 alters depending on external stimuli. This is consistent with previous studies showing that the *E. coli* aquaglyceroporin GlpF has different oligomerization states depending

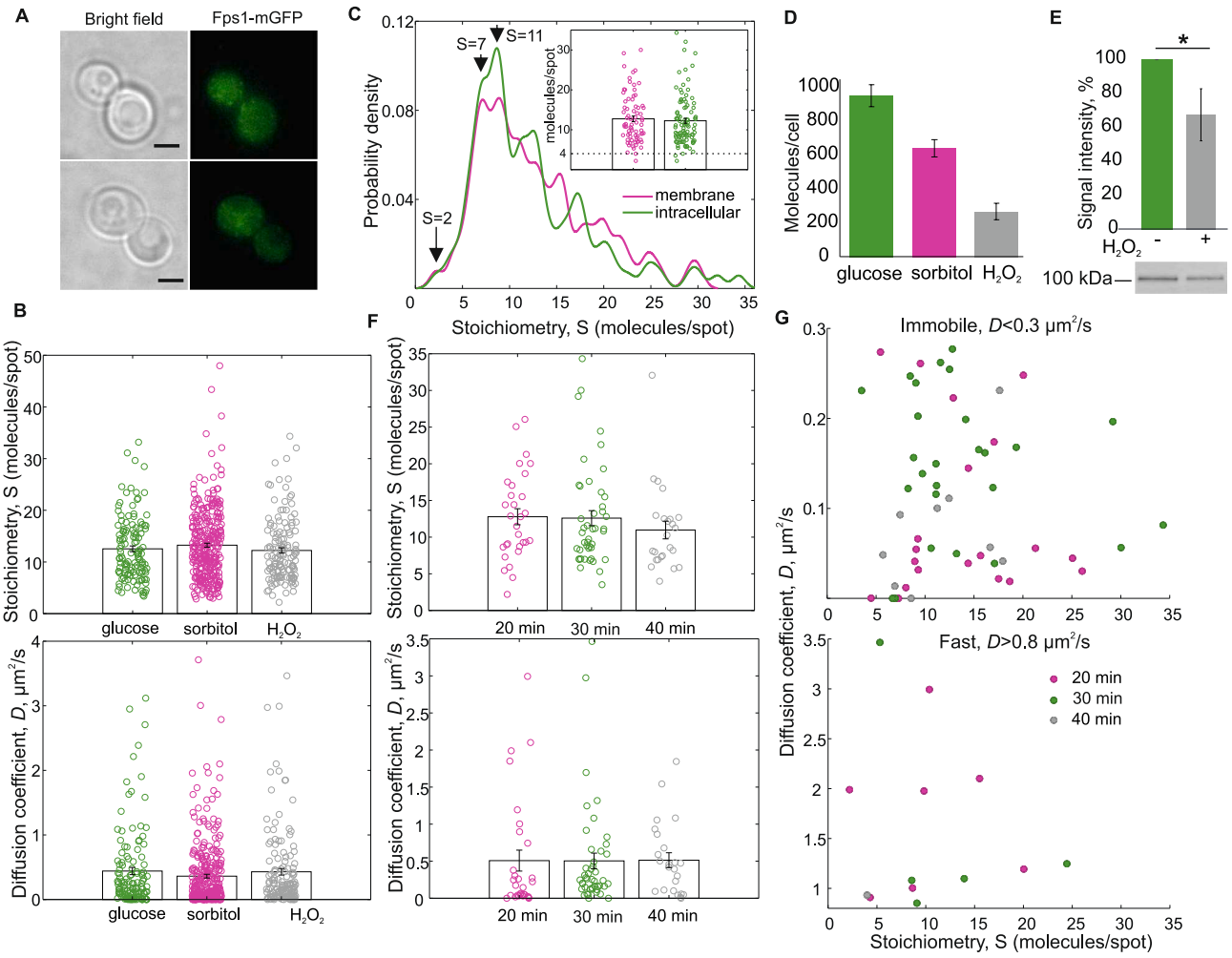

Fig. 4. A. Examples of Slimfield images of *S. cerevisiae* cells expressing genomically integrated Fps1-mGFP fusion upon oxidative stress: brightfield (left) and green channel (right) are shown. Scale bar 2 μm. B. Jitter plots of Fps1-mGFP stoichiometry (left) and diffusion coefficient (right) under various conditions. Standard error bards are shown). C. Kernel Density plot of the Fps1-mGFP stoichiometry distributions on the cellular membrane (magenta) and intracellular (green) spots. Inset: Jitter bar chart of membrane (magenta) and intracellular (green) Fps1-mGFP foci stoichiometry. Error bars represent standard error of mean. D. Numbers of Fps1 molecules per cell in yeast grown in standard (glucose, green), osmotic (sorbitol, magenta) or peroxide stress (H_2O_2, gray) conditions. Standard error bars are indicated. E. Western blot analysis of Fps1-mGFP levels in protein extracts from untreated cells or exposed to oxidative stress. Quantification of the signal was performed using Image-Studio Lite (LI-COR Biosciences) with local background normalization. Standard error bars are indicated. Student *t*-test, *p $<$ 0.05. One representative image of six replicates is shown. F. Jitter plots of Fps1-mGFP foci stoichiometry (top) and diffusion coefficients (bottom) in cells treated with hydrogen peroxide for 20 min (magenta), 30 min (green) or 40 min (gray). Error bars represent standard error of mean. G. Scatter plots of immobile (top) and fast moving (bottom) Fps1 foci in cells exposed to H_2O_2 for 20 min (magenta), 30 min (green) or 40 min (gray).

on salt concentration [79]. Rapid light microscopy approaches, such as those employed by us here, also permit investigating regulatory features on a single-molecule level which is difficult to achieve with traditional biochemical methods or standard epifluorescence imaging techniques. The key importance is correlating these molecular scale observations with changes to the microenvironment of individual cells. In doing so, we provide evidence that hyper-osmotic conditions and oxidative stress change the rates of Fps1 turnover compared to standard non-stress conditions. Moreover, we suggest that one of the steps in Fps1 degradation upon oxidative stress is the assembly of smaller foci into larger clusters. We also show, that inside the cell, Fps1 exists in an immobile state which might indicate its presence on membranes of intracellular organelles.

Our study provides novel insights into real-time MIPs dynamics within plasma membrane and in the rest of the cell. Further multicolor super-resolution millisecond approaches can be applied to the studied system to determine the machinery of channel interactions with associated proteins which regulate channel opening and closure or provide a binding scaffold, such as Sho1 protein scaffold for Fps1 [59,80].

6. Funding sources

This work has been supported by Adlerbertska forskningsstiftelsen, the Biological Physical Science institute (BPSI), the Royal Society Newton International Fellowship (grant number NF160208), EPSRC EP/T002166/1, BBSRC BB/R001235/1, Marie Curie EU FP7 ITN Ref 764591, and the Leverhulme Trust RPG-2019-156/RPG-2017-340.

CRediT authorship contribution statement

Sviatlana Shashkova: Methodology, Data curation, Formal analysis, Visualization, Software, Supervision, Validation, Project administration, Funding acquisition, Writing - original draft, Writing - review & editing. **Mikael Andersson:** Methodology, Conceptualization, Investigation, Data curation, Funding acquisition, Software, Formal analysis, Validation, Writing - original draft, Writing - review & editing. **Stefan Hohmann:** Methodology, Conceptualization, Funding acquisition, Writing - original draft. **Mark C. Leake:** Methodology, Resources, Supervision, Project administration, Funding acquisition, Writing -

original draft.

Acknowledgements

We thank Dr Adam Wollman, University of Newcastle, UK, for his assistance with the Slimfield data analysis.

Appendix A. Supplementary data

Supplementary data to this article can be found online at https://doi.org/10.1016/j.ymeth.2020.05.003.

References

[1] M.C. Leake, Analytical tools for single-molecule fluorescence imaging in cellulo, PCCP 16 (2014) 12635–12647, https://doi.org/10.1039/c4cp00219a.
[2] H. Miller, Z. Zhou, J. Shepherd, A. Wollman, M. Leake, Single-molecule techniques in biophysics: a review of the progress in methods and applications, Reports Prog. Phys. (2017), https://doi.org/10.1088/1361-6633/aa8a02.
[3] T. Lenn, M.C. Leake, Experimental approaches for addressing fundamental biological questions in living, functioning cells with single molecule precision, Open Biol. 2 (2012), 120090, https://doi.org/10.1098/rsob.120090.
[4] S. Shashkova, M.C. Leake, Single-molecule fluorescence microscopy review: shedding new light on old problems, BSR20170031, Biosci. Rep. 37 (2017), https://doi.org/10.1042/BSR20170031.
[5] M.C. Leake, The physics of life: one molecule at a time, Philos. Trans. R Soc. London B Biol. Sci. 368 (2012).
[6] J.R. Heath, A. Ribas, P.S. Mischel, Single-cell analysis tools for drug discovery and development, Nat. Rev. Drug Discov. 15 (2016) 204–216, https://doi.org/10.1038/nrd.2015.16.
[7] M.C. Leake, Shining the spotlight on functional molecular complexes: the new science of single-molecule cell biology, Commun. Integr. Biol. 3 (2010) 415–418, https://doi.org/10.4161/cib.3.5.12657.
[8] S.-W. Chiu, M.C. Leake, Functioning nanomachines seen in real-time in living bacteria using single-molecule and super-resolution fluorescence imaging, Int. J. Mol. Sci. 12 (2011) 2518–2542, https://doi.org/10.3390/ijms12042518.
[9] S. Shashkova, M.C. Leake, Systems biophysics: single-molecule optical proteomics in single living cells, Curr. Opin. Syst. Biol. 7 (2018), https://doi.org/10.1016/j.coisb.2017.11.006.
[10] A.J.M. Wollman, E.G. Hedlund, S. Shashkova, M.C. Leake, Towards mapping the 3D genome through high speed single-molecule tracking of functional transcription factors in single living cells, Methods 170 (2020) 82–89, https://doi.org/10.1016/j.ymeth.2019.06.021.
[11] A. Nenninger, G. Mastroianni, A. Robson, T. Lenn, Q. Xue, M.C. Leake, C. W. Mullineaux, Independent mobility of proteins and lipids in the plasma membrane of Escherichia coli, Mol. Microbiol. 92 (2014) 1142–1153, https://doi.org/10.1111/mmi.12619.
[12] J. Tam, D. Merino, Stochastic optical reconstruction microscopy (STORM) in comparison with stimulated emission depletion (STED) and other imaging methods, J. Neurochem. 135 (2015) 643–658, https://doi.org/10.1111/jnc.13257.
[13] Z. Liu, L.D. Lavis, E. Betzig, Imaging live-cell dynamics and structure at the single-molecule level, Mol. Cell 58 (2015) 644–659, https://doi.org/10.1016/j.molcel.2015.02.033.
[14] M. Stracy, A.J.M. Wollman, E. Kaja, J. Gapinski, J.-E. Lee, V.A. Leek, S.J. McKie, L. A. Mitchenall, A. Maxwell, D.J. Sherratt, M.C. Leake, P. Zawadzki, Single-molecule imaging of DNA gyrase activity in living *Escherichia coli*, Nucleic Acids Res. 47 (2019) 210–220, https://doi.org/10.1093/nar/gky1143.
[15] K.M. Giacomini, S.M. Huang, D.J. Tweedie, L.Z. Benet, K.L.R. Brouwer, X. Chu, A. Dahlin, R. Evers, V. Fischer, K.M. Hillgren, K.A. Hoffmaster, T. Ishikawa, D. Keppler, R.B. Kim, C.A. Lee, M. Niemi, J.W. Polli, Y. Sugiyama, P.W. Swaan, J. A. Ware, S.H. Wright, S. Wah Yee, M.J. Zamek-Gliszczynski, L. Zhang, Membrane transporters in drug development, Nat. Rev. Drug Disc. 9 (2010) 215–236, https://doi.org/10.1038/nrd3028.
[16] S. Shabala, J. Bose, A.T. Fuglsang, I. Pottosin, On a quest for stress tolerance genes: Membrane transporters in sensing and adapting to hostile soils, J. Exp. Bot. 67 (2016) 1015–1031, https://doi.org/10.1093/jxb/erv465.
[17] L. Chantranupong, R.L. Wolfson, D.M. Sabatini, Nutrient-sensing mechanisms across evolution, Cell 161 (2015) 67–83, https://doi.org/10.1016/j.cell.2015.02.041.
[18] M. Andersson, S. Hohmann, Yeast aquaporins and aquaglyceroporins: a matter of lifestyle, in: Aquaporins Heal. Dis. New Mol. Targets Drug Disc., CRC Press, 2016: pp. 77–100. https://doi.org/10.1201/b19017-7.
[19] M. Mollapour, P.W. Piper, Hog1 mitogen-activated protein kinase phosphorylation targets the yeast Fps1 aquaglyceroporin for endocytosis, thereby rendering cells resistant to acetic acid, Mol. Biol. Cell 27 (2007) 6446–6456, https://doi.org/10.1128/MCB.02205-06.
[20] R. Wysocki, C.C. Chéry, D. Wawrzycka, M. Van Hulle, R. Cornelis, J.M. Thevelein, M.J. Tamás, The glycerol channel Fps1p mediates the uptake of arsenite and antimonite in Saccharomyces cerevisiae, Mol. Microbiol. 40 (2001) 1391–1401, https://doi.org/10.1046/j.1365-2958.2001.02485.x.
[21] K. Luyten, J. Albertyn, W.F. Skibbe, B.A. Prior, J. Ramos, J.M. Thevelein, S. Hohmann, Fps1, a yeast member of the MIP family of channel proteins, is a facilitator for glycerol uptake and efflux and is inactive under osmotic stress, EMBO J. 14 (1995) 1360–1371, https://doi.org/10.1002/j.1460-2075.1995.tb07122.x.
[22] S.E. Beese-Sims, J. Lee, D.E. Levin, Yeast Fps1 glycerol facilitator functions as a homotetramer, Yeast 28 (2011) 815–819, https://doi.org/10.1002/yea.1908.
[23] R.K. Verma, A.B. Gupta, R. Sankararamakrishnan, Chapter twenty-three - major intrinsic protein superfamily: Channels with unique structural features and diverse selectivity filters, in: K.S. Arun (Ed.), Methods Enzymol., Academic Press, 2015, pp. 485–520, https://doi.org/https://doi.org/10.1016/bs.mie.2014.12.006.
[24] E. Kruse, N. Uehlein, R. Kaldenhoff, The aquaporins, Genome Biol. 7 (2006) 206, https://doi.org/10.1186/gb-2006-7-2-206.
[25] M. Plank, G.H. Wadhams, M.C. Leake, Millisecond timescale slimfield imaging and automated quantification of single fluorescent protein molecules for use in probing complex biological processes, Integr. Biol. (Camb) 1 (2009) 602–612, https://doi.org/10.1039/b907837a.
[26] R. Reyes-Lamothe, D.J. Sherratt, M.C. Leake, Stoichiometry and architecture of active DNA replication machinery in Escherichia coli, Science 328 (2010) 498–501, https://doi.org/10.1126/science.1185757.
[27] A.H. Syeda, A.J.M. Wollman, A.L. Hargreaves, J.A.L. Howard, J.-G. Brüning, P. McGlynn, M.C. Leake, Single-molecule live cell imaging of Rep reveals the dynamic interplay between an accessory replicative helicase and the replisome, Nucleic Acids Res. (2019), https://doi.org/10.1093/nar/gkz298.
[28] R. Heim, A.B. Cubitt, R.Y. Tsien, Improved green fluorescence, Nature 373 (1995) 663–664, https://doi.org/10.1038/373663b0.
[29] D.A. Zacharias, J.D. Violin, A.C. Newton, R.Y. Tsien, Partitioning of lipid-modified monomeric GFPs into membrane microdomains of live cells, Science (80-.) (2002) 296, https://doi.org/10.1126/science.1068539.
[30] S.E. Beese, T. Negishi, D.E. Levin, Identification of positive regulators of the yeast fps1 glycerol channel, PLoS Genet. 5 (2009), e1000738, https://doi.org/10.1371/journal.pgen.1000738.g001.
[31] J. Lee, W. Reiter, I. Dohnal, C. Gregori, S. Beese-Sims, K. Kuchler, G. Ammerer, D. E. Levin, MAPK Hog1 closes the S. cerevisiae glycerol channel Fps1 by phosphorylating and displacing its positive regulators, Genes Dev. 27 (2013) 2590–2601, https://doi.org/10.1101/gad.229310.113.
[32] E. Maciaszczyk-Dziubinska, I. Migdal, M. Migocka, T. Bocer, R. Wysocki, The yeast aquaglyceroporin Fps1p is a bidirectional arsenite channel, FEBS Lett. 584 (2010) 726–732, https://doi.org/10.1016/j.febslet.2009.12.027.
[33] A.J.M. Wollman, S. Shashkova, E.G. Hedlund, R. Friemann, S. Hohmann, M. C. Leake, Transcription factor clusters regulate genes in eukaryotic cells, Elife 6 (2017), e27451, https://doi.org/10.7554/eLife.27451.
[34] R.D. Gietz, R.H. Schiestl, Frozen competent yeast cells that can be transformed with high efficiency using the LiAc/SS carrier DNA/PEG method, Nat. Protoc. 2 (2007) 1–4, https://doi.org/10.1038/nprot.2007.17.
[35] A.J.M. Wollman, M.C. Leake, Millisecond single-molecule localization microscopy combined with convolution analysis and automated image segmentation to determine protein concentrations in complexly structured, functional cells, one cell at a time, Faraday Discuss. 184 (2015) 401–424, https://doi.org/10.1039/c5fd00077g.
[36] H. Miller, Z. Zhou, A.J.M. Wollman, M.C. Leake, Superresolution imaging of single DNA molecules using stochastic photoblinking of minor groove and intercalating dyes, Methods 88 (2015) 81–88, https://doi.org/10.1016/j.ymeth.2015.01.010.
[37] Y. Sun, A.J.M. Wollman, F. Huang, M.C. Leake, L.N. Liu, Single-organelle quantification reveals stoichiometric and structural variability of carboxysomes dependent on the environment, Plant Cell 31 (2019) 1648–1664, https://doi.org/10.1105/tpc.18.00787.
[38] M.C. Leake, J.H. Chandler, G.H. Wadhams, F. Bai, R.M. Berry, J.P. Armitage, Stoichiometry and turnover in single, functioning membrane protein complexes, Nature 443 (2006) 355–358, https://doi.org/10.1038/nature05135.
[39] S. Shashkova, A. Wollman, S. Hohmann, M.C. Leake, Characterising Maturation of GFP and mCherry of genomically integrated Fusions in Saccharomyces cerevisiae, Bio-Protocol 8 (2018), e2710, https://doi.org/10.21769/BioProtoc.2710.
[40] U.K. Laemmli, Cleavage of structural proteins during the assembly of the head of bacteriophage T4, Nature 227 (1970) 680–685, https://doi.org/10.1038/227680a0.
[41] J.-M. Verbavatz, D. Brown, I. Sabolić, G. Valenti, D.A. Ausiello, A.N. Van Hoek, T. Ma, A.S. Verkman, Tetrameric assembly of CHIP28 water channels in liposomes and cell membranes: a freeze-fracture study, J. Cell Biol. 123 (1993) 605–618, https://doi.org/10.1083/jcb.123.3.605.
[42] L.S. King, D. Kozono, P. Agre, From structure to disease: the evolving tale of aquaporin biology, Nat. Rev. Mol. Cell Biol. 5 (2004) 687–698, https://doi.org/10.1038/nrm1469.
[43] T. Braun, A. Philippsen, S. Wirtz, M.J. Borgnia, P. Agre, W. Kühlbrandt, A. Engel, H. Stahlberg, The 3.7 Å projection map of the glycerol facilitator GlpF: a variant of the aquaporin tetramer, EMBO Rep. 1 (2000) 183–189, https://doi.org/10.1093/embo-reports/kvd022.
[44] M.J. Borgnia, D. Kozono, G. Calamita, P.C. Maloney, P. Agre, Functional reconstitution and characterization of AqpZ, the E. coli water channel protein, J. Mol. Biol. 291 (1999) 1169–1179, https://doi.org/10.1006/jmbi.1999.3032.
[45] M.E. Van der Rest, A.H. Kamminga, A. Nakano, Y. Anraku, B. Poolman, W. N. Konings, The plasma membrane of Saccharomyces cerevisiae: Structure, function, and biogenesis, Microbiol. Rev. 59 (1995) 304–322, https://doi.org/10.1128/mmbr.59.2.304-322.1995.
[46] K. Fushimi, A.S. Verkman, Low viscosity in the aqueous domain of cell cytoplasm measured by picosecond polarization microfluorimetry, J. Cell Biol. 112 (1991) 719–725, https://doi.org/10.1083/JCB.112.4.719.

[47] C. Hachez, A. Besserer, A.S. Chevalier, F. Chaumont, Insights into plant plasma membrane aquaporin trafficking, Trends Plant Sci. 18 (2013) 344–352, https://doi.org/10.1016/j.tplants.2012.12.003.
[48] K. Takata, T. Matsuzaki, Y. Tajika, Aquaporins: water channel proteins of the cell membrane, Prog. Histochem. Cytochem. 39 (2004) 1–83, https://doi.org/10.1016/j.proghi.2004.03.001.
[49] Å. Valadi, K. Granath, L. Gustafsson, L. Adler, Distinct intracellular localization of Gpd1p and Gpd2p, the two yeast isoforms of NAD+-dependent glycerol-3-phosphate dehydrogenase, explains their different contributions to redox-driven glycerol production, J. Biol. Chem. 279 (2004) 39677–39685, https://doi.org/10.1074/jbc.M403310200.
[50] M. Klein, S. Swinnen, J.M. Thevelein, E. Nevoigt, Glycerol metabolism and transport in yeast and fungi: established knowledge and ambiguities, Environ. Microbiol. 19 (2017) 878–893, https://doi.org/10.1111/1462-2920.13617.
[51] L. Klug, G. Daum, Yeast lipid metabolism at a glance, FEMS Yeast Res. 14 (2014) 369–388, https://doi.org/10.1111/1567-1364.12141.
[52] H. Sugiya, M. Matsuki-Fukushima, S. Hashimoto, Role of aquaporins and regulation of secretory vesicle volume in cell secretion, J. Cell Mol. Med. 12 (2008) 1486–1494, https://doi.org/10.1111/j.1582-4934.2008.00239.x.
[53] L.A. Coury, M. Hiller, J.C. Mathai, E.W. Jones, M.L. Zeidel, J.L. Brodsky, Water Transport across Yeast Vacuolar and Plasma Membrane-Targeted Secretory Vesicles Occurs by Passive Diffusion, J. Bacteriol. 181 (1999) 4437, https://doi.org/10.1128/JB.181.14.4437-4440.1999.
[54] S. Sugiyama, M. Tanaka, Distinct segregation patterns of yeast cell-peripheral proteins uncovered by a method for protein segregatome analysis, Proc. Natl. Acad. Sci. U. S. A. 116 (2019) 8909–8918, https://doi.org/10.1073/pnas.1819715116.
[55] M.J. Tamás, K.S. Luyten, F.C. Hernandez, A. Albertyn, J. Valadi, H. Li, H. Prior, B. A. Kilian, S.G. Ramos, J. Gustafsson, L. Thevelein, J.M. Hohmann, Fps1p controls the accumulation and release of the compatible solute glycerol in yeast osmoregulation, Mol. Microbiol. 31 (1999) 1087–1104, https://doi.org/10.1046/j.1365-2958.1999.01248.x.
[56] S.R. Talemi, C.F. Tiger, M. Andersson, R. Babazadeh, N. Welkenhuysen, E. Klipp, S. Hohmann, J. Schaber, Systems level analysis of the yeast osmo-stat, Sci. Rep. 6 (2016) 30950, https://doi.org/10.1038/srep30950.
[57] A. Miermont, F. Waharte, S. Hu, M.N. McClean, S. Bottani, S. Léon, P. Hersen, Severe osmotic compression triggers a slowdown of intracellular signaling, which can be explained by molecular crowding, Proc. Natl. Acad. Sci. U. S. A. 110 (2013) 5725–5730, https://doi.org/10.1073/pnas.1215367110.
[58] A.J. Boersma, I.S. Zuhorn, B. Poolman, A sensor for quantification of macromolecular crowding in living cells, Nat. Methods 12 (2015) 227–229, https://doi.org/10.1038/nmeth.3257.
[59] M.H.Y. Lam, J. Snider, M. Rehal, V. Wong, F. Aboualizadeh, L. Drecun, O. Wong, B. Jubran, M. Li, M. Ali, M. Jessulat, V. Deineko, R. Miller, M. eum Lee, H.-O. Park, A. Davidson, M. Babu, I. Stagljar, A comprehensive membrane interactome mapping of Sho1p reveals Fps1p as a novel key player in the regulation of the HOG pathway in S. cerevisiae, J. Mol. Biol. 427 (2015) 2088–2103, https://doi.org/10.1016/j.jmb.2015.01.016.
[60] A. Muir, F.M. Roelants, G. Timmons, K.L. Leskoske, J. Thorner, Down-regulation of TORC2-Ypk1 signaling promotes MAPK-independent survival under hyperosmotic stress, Elife. 4 (2015), https://doi.org/10.7554/eLife.09336.
[61] D. Ahmadpour, E. Maciaszczyk-Dziubinska, R. Babazadeh, S. Dahal, M. Migocka, M. Andersson, R. Wysocki, M.J. Tamás, S. Hohmann, The mitogen-activated protein kinase Slt2 modulates arsenite transport through the aquaglyceroporin Fps1, FEBS Lett. 590 (2016) 3649–3659, https://doi.org/10.1002/1873-3468.12390.
[62] Y.C. Kim, R.B. Best, J. Mittal, Macromolecular crowding effects on protein-protein binding affinity and specificity, J. Chem. Phys. 133 (2010), 205101, https://doi.org/10.1063/1.3516589.
[63] G.P. Bienert, F. Chaumont, Aquaporin-facilitated transmembrane diffusion of hydrogen peroxide, Biochim. Biophys. Acta - Gen. Subj. 1840 (2014) 1596–1604, https://doi.org/10.1016/j.bbagen.2013.09.017.
[64] D. Aguayo, N. Pacheco, E.H. Morales, B. Collao, R. Luraschi, C. Cabezas, P. Calderón, F. González-Nilo, F. Gil, I.L. Calderón, C.P. Saavedra, Hydrogen peroxide and hypochlorous acid influx through the major S. Typhimurium porin OmpD is affected by substitution of key residues of the channel, Arch. Biochem. Biophys. 568 (2015) 38–45, https://doi.org/10.1016/j.abb.2015.01.005.
[65] Y. Boursiac, J. Boudet, O. Postaire, D.T. Luu, C. Tournaire-Roux, C. Maurel, Stimulus-induced downregulation of root water transport involves reactive oxygen species-activated cell signalling and plasma membrane intrinsic protein internalization, Plant J. 56 (2008) 207–218, https://doi.org/10.1111/j.1365-313X.2008.03594.x.
[66] S.E. Fligiel, E.C. Lee, J.P. McCoy, K.J. Johnson, J. Varani, Protein degradation following treatment with hydrogen peroxide, Am. J. Pathol. 115 (1984) 418–425.
[67] Y. Klemes, D. Godinger, J. Aronovitch, Temporary exposure to hydrogen peroxide increases intracellular protein degradation in E. coli, FEMS Microbiol. Lett. 44 (1987) 277–282, https://doi.org/10.1111/j.1574-6968.1987.tb02282.x.
[68] H.M. Semchyshyn, O.B. Abrat, J. Miedzobrodzki, Y. Inoue, V.I. Lushchak, Acetate but not propionate induces oxidative stress in bakers' yeast Saccharomyces cerevisiae, Redox Rep. 16 (2011) 15–23, https://doi.org/10.1179/174329211X12968219310954.
[69] A. Veerappan, F. Cymer, N. Klein, D. Schneider, The Tetrameric α-Helical Membrane Protein GlpF Unfolds via a Dimeric Folding Intermediate, Biochemistry 50 (2011) 10223–10230, https://doi.org/10.1021/bi201266m.
[70] W. Kammerloher, U. Fischer, G.P. Piechottka, A.R. Schäffner, Water channels in the plant plasma membrane cloned by immunoselection from a mammalian expression system, Plant J. 6 (1994) 187–199, https://doi.org/10.1046/j.1365-313X.1994.6020187.x.
[71] M.J. Daniels, T.E. Mirkov, M.J. Chrispeels, The plasma membrane of Arabidopsis thaliana contains a mercury-insensitive aquaporin that is a homolog of the tonoplast water channel protein TIP, Plant Physiol. 106 (1994) 1325–1333, https://doi.org/10.1104/pp.106.4.1325.
[72] L.M. Barone, H.H. Mu, C.J. Shih, K.B. Kashlan, B.P. Wasserman, Distinct biochemical and topological properties of the 31- and 27-kilodalton plasma membrane intrinsic protein subgroups from red beet, Plant Physiol. 118 (1998) 315–322, https://doi.org/10.1104/pp.118.1.315.
[73] G.P. Bienert, D. Cavez, A. Besserer, M.C. Berny, D. Gilis, M. Rooman, F. Chaumont, A conserved cysteine residue is involved in disulfide bond formation between plant plasma membrane aquaporin monomers, Biochem. J. 445 (2012) 101–111, https://doi.org/10.1042/BJ20111704.
[74] S.J. Singer, G.L. Nicolson, The fluid mosaic model of the structure of cell membranes, Science (80-) 175 (1972) 720–731, https://doi.org/10.1126/science.175.4023.720.
[75] T. Lang, S.O. Rizzoli, Membrane protein clusters at nanoscale resolution: more than pretty pictures, Physiology 25 (2010) 116–124, https://doi.org/10.1152/physiol.00044.2009.
[76] J.B. de la Serna, G.J. Schütz, C. Eggeling, M. Cebecauer, There is no simple model of the plasma membrane organization, Front. Cell Dev. Biol. 4 (2016) 106, https://doi.org/10.3389/fcell.2016.00106.
[77] T.C. Walther, J.H. Brickner, P.S. Aguilar, S. Bernales, C. Pantoja, P. Walter, Eisosomes mark static sites of endocytosis, Nature 439 (2006) 998–1003, https://doi.org/10.1038/nature04472.
[78] K. Choudhuri, M.L. Dustin, Signaling microdomains in T cells, FEBS Lett. 584 (2010) 4823–4831, https://doi.org/10.1016/j.febslet.2010.10.015.
[79] M.J. Borgnia, P. Agre, Reconstitution and functional comparison of purified GlpF and AqpZ, the glycerol and water channels from Escherichia coli, Proc Natl Acad Sci U S A. 98 (2001) 2888–2893, https://doi.org/10.1073/pnas.051628098.
[80] K. Tatebayashi, K. Yamamoto, M. Nagoya, T. Takayama, A. Nishimura, M. Sakurai, T. Momma, H. Saito, Osmosensing and scaffolding functions of the oligomeric four-transmembrane domain osmosensor Sho1, Nat. Commun. 6 (2015) 1–15, https://doi.org/10.1038/ncomms7975.